CHAPTER 7

THEORIES OF BEARING CAPACITY AND SETTLEMENT

7.1 INTRODUCTION

Testing of soil in the laboratory, and perhaps in the field, to obtain properties is required to allow the computation of bearing capacity and settlement. The reader is referred to Chapter 3 for details on the determination of the required parameters of the soil at a site.

The problems to be addressed in this chapter can be illustrated by the shallow foundation of given lateral dimensions resting on soil, as shown in Figure 7.1a. The first of two problems facing the engineer is to find the unit vertical load on a shallow foundation, or on the base of a deep foundation, that will cause the foundation to settle precipitously or to collapse. The unit load at failure is termed the *bearing capacity.* With regard to bearing capacity, the following comments are pertinent:

1. Any deformation of the foundation itself is negligible or disregarded.
2. The stress-strain curve for the soil is as shown in Figure 7.1b.
3. The base of the foundation may be smooth or rough.
4. The soil is homogeneous through the semi-infinite region along and below the foundation.
5. The loading is increased slowly with no vibration.
6. There is no interaction with nearby foundations. In spite of the constraints on computing the values, the concept of bearing capacity has been used for the design of foundations for decades and presently remains in extensive use.

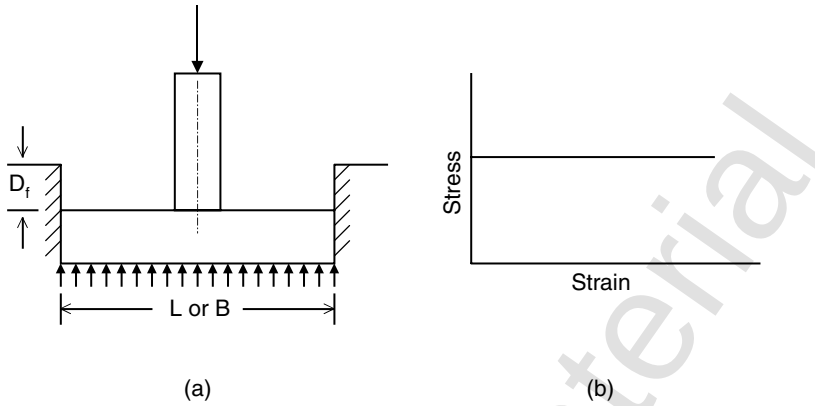

Figure 7.1 Example of footing and stress-strain curve used in developing bearing-capacity equations.

Investigators have noted that the bearing capacity equations will vary if the failure is *general* where symmetrical failure surfaces develop below the base of the foundation; is *local* where a failure occurs due to excessive settlement of the foundation; or is a *punch-through* where the foundation punches through a strong surface layer and causes the weak soil below to fail. The equations for general shear failure are most important.

The second of the two problems addressed here is the computation of settlement of a foundation such as that shown in Figure 7.1. Two types of settlement are noted: immediate or short-term settlement and long-term settlement due to the consolidation of saturated clays. The immediate settlement of foundations on sands of loose or medium density is relatively so large that settlement controls, termed a *local shear failure,* as noted above, and a general bearing capacity failure does not occur. Immediate settlement of foundations on sand and clay is discussed in Chapter 9.

Equations and procedures for dealing with long-term settlement due to consolidation are presented here. The settlement of deep foundations is discussed in chapters that deal specifically with piles and drilled shafts.

The finite-element method (FEM) discussed in Chapter 5 provides valuable information to the engineer on both bearing capacity and settlement, as demonstrated by the example solution presented. FEM can now be implemented on most personal computers, rather than on large mainframes, and will play a much greater role in geotechnical engineering as methods for modeling the behavior of soil are perfected. Leshchinsky and Marcozzi (1990) performed small-scale experiments with flexible and rigid footings and noted that the flexible footings performed better than the rigid ones. Rather than use the performance of expensive tests with full-sized footings, FEM can be used to study the flexibility of footings.

7.2 TERZAGHI'S EQUATIONS FOR BEARING CAPACITY

The equations developed by Terzaghi (1943) have been in use for a long time and continue to be used by some engineers. His development made use of studies by Rankine (1857), Prandtl (1920), and Reissner (1924). The two-dimensional model employed by Terzaghi (Figure 7.2) was a long strip footing with a width of $2B$ (later, authors simply use B for the width of footing) and a depth of the base of the footing below the ground surface of D_f. The base of the footing was either smooth or rough, with the shape of the solution for a rough footing shown in the figure. The wedge a, b, d is assumed to move down with the footing, the surface d, e is defined by a log spiral and the soil along that surface is assumed to have a failure in shear, and the zone a, e, f is assumed to be in a plastic state defined by the Rankine equation.

The equations developed by Terzaghi for bearing capacity factors are as follows:

$$Q_D = 2B(cN_c + \gamma D_f N_q + \gamma B N_\gamma) \quad \text{(general shear failure)} \tag{7.1}$$

$$Q'_D = 2B(\tfrac{2}{3}\, cN'_c + \gamma B N'_\gamma + \gamma B N'_\gamma) \quad \text{(local shear failure)} \tag{7.2}$$

where

Q_D = load at failure of the strip footing,
c = cohesion intercept,
γ = unit weight of soil, and
$N_c, N'_c, N_q, N'_q, N_\gamma, N'_\gamma$ = bearing capacity factors shown graphically in Figure 7.3.

The differences in settlement for a general shear failure and a local shear failure are shown in Figure 7.4, where the general shear failure is depicted by the solid line. The footing on loose soil is expected to settle a large amount compared to the footing on dense soil, which Terzaghi elected to reflect by

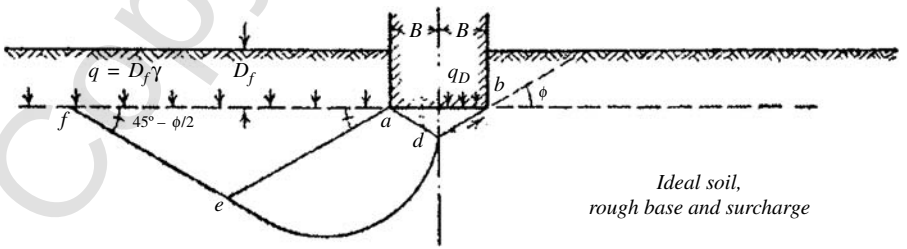

Figure 7.2 Model used by Terzaghi in developing valves for bearing-capacity factors (from Terzaghi, 1943, p. 121).

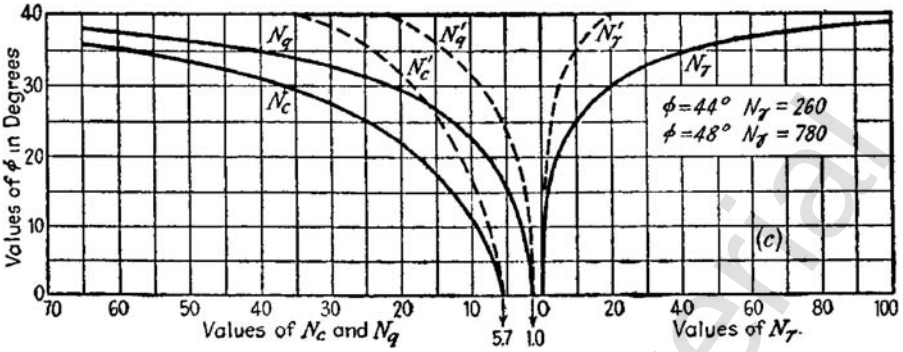

Figure 7.3 Terzaghi's bearing-capacity factors (from Terzaghi, 1943, p. 125).

reducing the values of the bearing capacity factors for loose soil. A proposed reduction in bearing capacity to deal with excessive settlement is disregarded here because Chapter 9 deals with short-term settlement of shallow foundations. The engineer may reduce the load on the foundation if the immediate settlement is deemed excessive.

7.3 REVISED EQUATIONS FOR BEARING CAPACITY

A number of authors have made proposals for bearing capacity factors, including Caquot and Kérisel (1953), Meyerhof (1963), Hansen and Christensen (1969), Hansen (1970), and Vesić (1973). The basic form of the bearing-capacity equation (Eq. 7.1), proposed by Terzaghi, has been accepted by most subsequent investigators; however, two modifications have been suggested: (1) improved analysis of the model proposed by Terzaghi (Figure 7.2), and

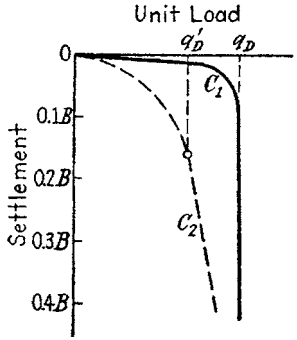

Figure 7.4 Assumed curves for unit load versus settlement for a footing on dense soil, C_1 and on loose soil, C_2 (from Terzaghi, 1943, p. 118).

(2) an extension of the method to include a number of factors such as inclined loading and a rectangular footing rather than a strip.

In addition, a number of other studies have been undertaken, such as those using FEM, to study the upper- and lower-bound values of the bearing capacity (Ukritchon et al., 2003). Hansen's method has been selected and is presented in detail because it is comprehensive and because the analytical results agree reasonably well with experimental results.

7.4 EXTENDED FORMULAS FOR BEARING CAPACITY BY J. BRINCH HANSEN

Hansen employed the same basic equation as Terzaghi except that the width of the footing is B instead of $2B$ as employed by Terzaghi. Hansen's basic equation is

$$\frac{Q_d}{B} = \frac{1}{2}\gamma B N_\gamma + \gamma D_f N_q + cN_c \tag{7.3}$$

where

Q_d = ultimate bearing capacity,
B = width of foundation, and
γ = unit weight of soil (use γ' for submerged unit weight).

The equations below are for the bearing-capacity factors N_q and N_c as expressed by exact formulas developed by Prandtl (1920):

$$N_q = e^{\pi \tan\phi} \tan^2\left(45 + \frac{\phi}{2}\right) \tag{7.4}$$

$$N_c = (N_q - 1)\cot\phi \tag{7.5}$$

(Note: if $\phi = 0$, $N_c = \pi + 2$.)

Hansen and Christensen (1969) presented a graph for N_γ as a function of the friction angle, δ, between the base of the footing and the sand (Figure 7.5). If the base is rough, $\delta = \phi$, and the values can be read from the indicated curve in Figure 7.5. Footings with a rough base, as would occur with concrete poured on a base of sand, are usually assumed in design. One of the authors witnessed construction in Moscow where concrete footings were in a plant and were being trucked to the job site. Extremely low temperatures for many months prevent casting of concrete in the field. If a designer wishes to account for low friction between the base of a footing and the sand, the curves in Figure 7.5 may be used, with the values for $\delta = 0$ indicating a perfectly

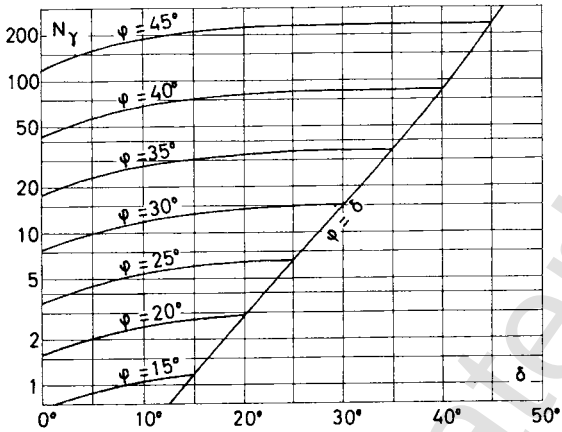

Figure 7.5 Bearing-capacity factor N_γ found for strip footings as a function of friction angles φ for sand and δ for subsurface of footing (from Hansen and Christensen, 1969).

smooth footing. The following equation is for a perfectly rough footing and is commonly used in design:

$$N_\gamma = 1.5(N_q - 1)\cot \phi \tag{7.6}$$

Hansen's bearing-capacity factors for the strip footing are presented in graphical form in Figure 7.6 and tabulated in Table 7.1. Perhaps Hansen's most important contribution was to extend the equations for bearing capacity

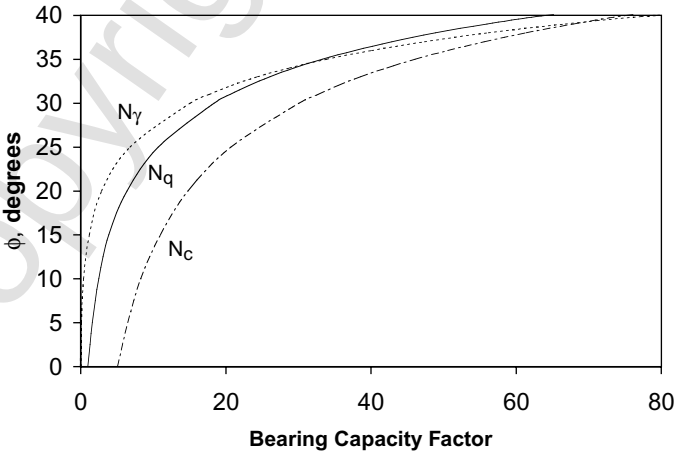

Figure 7.6 Hansen's bearing-capacity factors.

TABLE 7.1 Hansen's Bearing-Capacity Factors

ϕ (degrees)	N_q	N_c	N_γ
0	1.0	1.5	0.0
5	1.6	6.5	0.1
10	2.5	8.3	0.4
15	3.9	11.0	1.2
20	6.4	14.8	2.9
25	10.7	20.7	6.8
30	18.4	30.1	15.1
31	20.6	32.7	17.7
32	23.2	35.5	20.8
33	26.1	38.6	24.4
34	29.4	42.2	28.8
35	33.3	46.1	33.9
36	37.8	50.6	40.1
37	42.9	55.6	47.4
38	48.9	61.4	56.2
39	56.0	67.9	66.8
40	64.2	75.3	79.5
42	85.4	93.7	114.0
44	115.3	118.4	165.6
46	158.5	152.1	244.6
48	222.3	199.3	368.7
50	319.1	266.9	568.6

to deal with deviations from the simple case of a strip footing. The load may be eccentric, inclined, or both. The base of the foundation is usually placed at depth D_f below the ground surface. The foundation always has a limited length L and its shape may not be rectangular. Finally, the base of the foundation and the ground surface may be inclined. The equation for Hansen's extended formula is

$$\frac{Q_d}{A} = \frac{1}{2}\gamma B N_\gamma s_\gamma d_\gamma i_\gamma b_\gamma g_\gamma + \gamma D_f N_q s_q d_q i_q b_q g_q + c N_c s_c d_c i_c b_c g_c \quad (7.7)$$

where

A = area of footing,
s = shape factors,
d = depth factors,
i = inclination factors,
b = base inclination factors, and
g = ground inclination factors.

In the special case where $\phi = 0$, Hansen writes that it is theoretically more correct to introduce additive factors, and Eq. 7.8 presents the result:

$$\frac{Q_d}{A} = (\pi + 2)s_u(1 + s_c^a + d_c^a - i_c^a - b_c^a - g_c^a) \tag{7.8}$$

where s_u = undrained shear strength of the clay. The definitions of the modification factors are shown in the following sections. Hansen stated that when the modifications occur one at a time, a simple analytical solution or results from experiments can be used; however, when all of the factors are used together for more complicated cases, the resulting computation will be an approximation.

All of the loads acting above the base of the foundation are to be combined into one resultant, with a vertical component, V, acting normal to the base and a horizontal component H acting in the base. To account for eccentric loading, the foundation is re-configured so that the resultant intersects the base at a point called the *load center.* If the foundation has an irregular shape, a rectangular foundation meeting the above conditions is employed.

7.4.1 Eccentricity

With regard to eccentric loading on a shallow foundation, Hansen recommended that the foundation be reconfigured so that the eccentricity is eliminated on the foundation to be analyzed. The scheme proposed by Hansen is shown in Figure 7.7, where the original foundation is indicated by the solid lines. The point of application of the loading on the base of the foundation

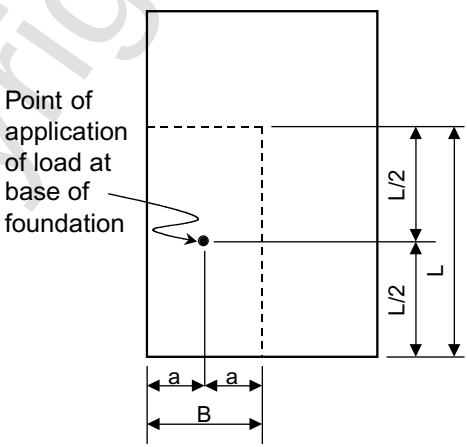

Figure 7.7 Sketch showing reconfiguration of the shape of a foundation to account for eccentric loading.

is shown by the dot, and the foundation to be analyzed is shown by the dashed lines. The eccentricity is exaggerated for purposes of illustration.

For foundations of other shapes with eccentric loads, the best possible rectangular foundation is configured with no eccentricity to replace the particular shape.

7.4.2 Load Inclination Factors

An inclination of the load will always mean a reduced bearing capacity, and solutions can be developed by revising the model shown in Figure 7.2. The following simple empirical formulas were proposed by Hansen:

$$i_q = \left[1 - 0.5 \frac{H}{(V + Ac \cot \phi)}\right]^5 \tag{7.9}$$

$$i_\gamma = \left[1 - 0.7 \frac{H}{(V + Ac \cot \phi)}\right]^5 \tag{7.10}$$

For the case where $\phi = 0$, the following equation may be used:

$$i_c^a = 0.5 - 0.5 \left(1 - \frac{H}{As_u}\right)^{0.5} \tag{7.11}$$

where

H = component of the load parallel to the base and
V = component of the load perpendicular to the base.

Equations 7.9 and 7.10 may not be used if the quantity inside the brackets becomes negative.

The above equations are valid for a horizontal force where H is equal to H_B that acts parallel to the short sides B of the equivalent effective rectangle. If H_B is substituted for H, the computed factors may be termed i_{qB}, $i_{\gamma B}$, and i_{cB}^a. In the more general case, a force component H_L also exists, acting parallel with the long sides L. Another set of factors may be computed by substituting H_L for H, and factors will result that may be termed i_{qL}, $i_{\gamma L}$, and i_{cL}^a. The first set of factors with the second subscript B may be used to investigate possible failure along the long sides L, and the second set of factors with the second subscript L may be used to investigate possible failure along the short sides B. One of the sets of analyses will control the amount of load that may be sustained by the foundation.

7.4.3 Base and Ground Inclination

The sketches in Figure 7.8 defined the inclination v of the base of the foundation and the inclination β of the ground. In the case of $\phi = 0$, the following equations were found:

$$b_c^a = \frac{2v}{\pi + 2} = \frac{v}{147} \tag{7.12}$$

$$g_c^a = \frac{2\beta}{\pi + 2} = \frac{\beta}{147} \tag{7.13}$$

where v, β, and 147 are in degrees.

For values of ϕ other than zero, the following equation applies:

$$b_q = e^{-2v\tan\phi} \tag{7.14}$$

Equations 7.11 through 7.13 may be used for only positive values of v and β, with β smaller than ϕ, and v plus β must not exceed 90°.

7.4.4 Shape Factors

Hansen recommended the following equations to deal with footings with rectangular shapes:

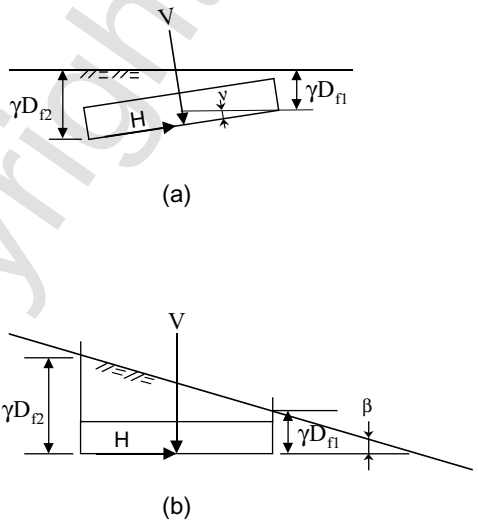

Figure 7.8 Sketches defining inclinations (a) of base v and (b) of ground β (from Hansen, 1970).

$$s_\gamma = 1 - 0.4\frac{B}{L} \tag{7.15}$$

$$s_q = 1 + \sin\phi\frac{B}{L} \tag{7.16}$$

$$s_c^a = 0.2\frac{B}{L} \tag{7.17}$$

The above shape factors are only for vertical loads. For inclined loads, formulas must be introduced to account for the inclination. Failure may occur along the long sides or along the short sides; thus, two sets of equations are required.

$$s_{cB}^a = 0.2 i_{cB}^a \frac{B}{L} \tag{7.18}$$

$$s_{cL}^a = 0.2 i_{cL}^a \frac{L}{B} \tag{7.19}$$

$$s_{qB} = 1 + \sin\phi\frac{Bi_{qB}}{L} \tag{7.20}$$

$$s_{qL} = 1 + \sin\phi\frac{Li_{qL}}{B} \tag{7.21}$$

$$s_{\gamma B} = 1 - 0.4\frac{Bi_{\gamma B}}{Li_{\gamma L}} \tag{7.22}$$

$$s_{\gamma L} = 1 - 0.4\frac{Li_{\gamma L}}{Bi_{\gamma B}} \tag{7.23}$$

For Eqs. 7.22 and 7.23, the special rule must be followed that a value exceeding 0.6 must always be used.

7.4.5 Depth Effect

Foundations are always placed at depth D_f below the ground surface, so the term γD_f is used to indicate the soil above the base of the foundation. The shear strength of the overburden soil is assumed to be the same as that of the soil below the base of the footing. If the overburden soil is weaker than the foundation soil, the depth effect may be reduced or ignored entirely.

7.4.6 Depth Factors

The depth factor for the effect of the weight of the soil is always equal to unity:

$$d_\gamma = 1 \tag{7.24}$$

For values of D_f that are small with respect to B, the following equations may be used:

$$d_c^a = 0.4 \frac{D_f}{B} \tag{7.25}$$

$$d_q = 1 + 2 \tan \phi(1 - \sin \phi)^2 \frac{D_f}{B} \tag{7.26}$$

When D_f is large with respect to B, the following equations were proposed by Hansen:

$$d_c^a = 0.4 \arctan \frac{D_f}{B} \tag{7.27}$$

$$d_q = 1 + 2 \tan \phi(1 - \sin \phi)^2 \arctan \frac{D_f}{B} \tag{7.28}$$

To test the formulas for large values of D_f/B, the following result was found:

$$\frac{Q_d}{A} = (\pi + 2)c_u\left(1 + 0.02 + 0.4 \frac{\pi}{2}\right) = 9.4c_u \tag{7.29}$$

The result in Eq. 7.29 agrees with the well-known value found for the resistance of the tip for piles founded in clay. The following formula applies for other values of friction angles:

$$\frac{Q_d}{A} = \gamma D_f N_q (1 + \sin \phi)[1 + \pi \tan \varphi(1 - \sin \phi)^2] \tag{7.30}$$

Hansen noted that for friction angles between 30° and 40° the above equation yields results in good agreement with the Danish experience for point resistance for piles in sand, provided that ϕ is taken as the friction angle in plane strain.

For the usual case of failure along the long sides L on the base, Eqs. 7.29 and 7.30 may be used with Eqs. 7.25 and 7.26, yielding values of the depth factors d_{cB}^a and d_{qB}. For the investigation of a possible failure along the short sides, B, equations for another set of depth factors must be used:

$$d_{cL}^{a} = 0.4 \arctan \frac{D_f}{L} \tag{7.31}$$

$$d_{qL} = 1 + 2 \tan \varphi(1 - \sin \phi)^2 \arctan \frac{D_f}{L} \tag{7.32}$$

7.4.7 General Formulas

In many instances, the horizontal force will have a component H_B parallel with the short sides B and a component H_L parallel with the long sides L, and the following formulas must be used:

$$\frac{Q_d}{A} \leq \frac{1}{2} \gamma N_\gamma B s_{\gamma B} i_{\gamma B} b_\gamma + (\gamma D_f + c \cot \phi) N_q d_{qB} s_{qB} i_{qB} b_q - c \cot \phi \tag{7.33a}$$

or

$$\frac{Q_d}{A} \leq \frac{1}{2} \gamma N_\gamma B s_{\gamma L} i_{\gamma L} b_\gamma + (\gamma D_f + c \cot \phi) N_q d_{qL} s_{qL} i_{qL} b_q - c \cot \phi \tag{7.33b}$$

The above equations may be used as follows. Of the two possibilities for the terms including γ, the upper term should be used when $Bi_{\gamma B} \leq Li_{\gamma L}$ and the lower term should be used when $Bi_{\gamma B} \geq Li_{\gamma L}$. A check on the proper choice is that $s_\gamma \geq 0.6$. Of the two possibilities for the terms including γD_f, the one giving the smallest value must always be chosen.

In the special case where $\phi = 0$, the smallest of the values from the following two equations may be used:

$$\frac{Q_d}{A} \leq (\pi + 2) c_u (1 + s_{cB}^{a} + d_{cB}^{a} - i_{cB}^{a} - b_c^{a} - g_c^{a}) \tag{7.34a}$$

or

$$\frac{Q_d}{A} \leq (\pi + 2) c_u (1 + s_{cL}^{a} + d_{cL}^{a} - i_{cL}^{a} - b_c^{a} - g_c^{a}) \tag{7.34b}$$

7.4.8 Passive Earth Pressure

If sufficient lateral movements of a footing occur to develop passive earth pressure on the edge of the footing, the bearing-capacity equations will be affected. Hansen's studies showed that the movements necessary to develop bearing capacity and passive earth pressure are of the same order of magnitude. The movement associated with bearing capacity is discussed in Chapter 9. In special cases, the movements required to develop bearing capacity and passive earth pressure can be computed by FEM.

With respect to design, for mainly vertical loads no passive pressure is employed. For mainly horizontal loads, passive pressure must be employed; however, the details of construction play an important role. If an oversized excavation is made for the foundation, the nearby soil may have been disturbed and/or the backfill may have been placed poorly so that passive earth pressure does not develop.

7.4.9 Soil Parameters

In the case of saturated clays, the relevant value c_u of undrained shear strength must be employed for short-term behavior; for long-term behavior, the parameters ϕ and c must be employed as determined from drained triaxial tests.

For sand, c can be assumed to equal zero. The equations shown in the sections above are based on the friction angle in plane strain. The following identity is recommended:

$$\phi_{pl} = 1.1\phi_{tr} \tag{7.35}$$

where

ϕ_{pl} = friction angle for plane strain conditions, and
ϕ_{tr} = friction angle determined from triaxial tests.

7.4.10 Example Computations

Examples from Hansen (1970) The results from two tests of a foundation on sand were reported by Muhs and Weib (1969). The shallow foundation had a length of 2 m and a width of 0.5 m. The water table was at the ground surface, the submerged unit weight of the sand was 0.95 t/m^3, the friction angle measured by the triaxial test was 40° to 42°, and the base of the footing was 0.5 m below the ground surface. In the first test the foundation was loaded centrally and vertically, and failure occurred as a load of 190 t. Hansen suggested the use of ϕ_{tr} of 40° in his discussion of the Muhs-Weib tests.

$$\phi_{pl} = 1.1(40) = 44°$$

Eq. 7.4: $$N_q = (20.78)(5.55) = 115.3$$

Eq. 7.6: $$N_\gamma = (1.5)(114.3)(0.9657) = 165.6$$

Using the first two terms of the Eq. 7.33, failure along the short sides, with no inclined loading, inclined soil surface, or cohesion, and noting that $d_\gamma = 1$.

$$\frac{D_d}{A} = \frac{1}{2}\gamma N_\gamma B s_{\gamma B} + \gamma D_f N_q d_{qB} s_{qB}$$

Eq. 7.16: $$s_{\gamma B} = 1 - 0.4\frac{0.5}{2} = 0.90$$

Eq. 7.17: $$s_{qB} = 1 + (0.695)\frac{0.5}{2} = 1.174$$

Eq. 7.29: $$d_{qB} = 1 + 2(0.966)(0.0932)(0.785) = 1.141$$

$$Q_d = 1\left(\frac{1}{2}(0.95)(0.5)(165.6)(0.90)(1) + (0.95)(0.5)(115.3)(1.174)(1.141)\right)$$
$$= 35.4 + 73.4 = 108.8t$$

The second test was performed with a foundation of the same size, in the same soil and position as the water table. The foundation was loaded centrally to failure with a vertical component $V = 108$ t and a horizontal component in the L direction $H_L = 39$ t. The revised Eq. 7.7 for the loading indicated is

$$\frac{Q_d}{A} = \frac{1}{2}\gamma L N_\gamma s_{\gamma L} d_{\gamma L} i_{\gamma L} + \gamma D_f N_q s_{qL} d_{qL} i_{qL};$$

because $H_B = 0$; $d_{qB} = 1.414$; $s_{qB} = 1.174$; $i_{\gamma B} = i_{qB} = 1$; $Bi_{\gamma B} = 0.5$; then $d_{qB} s_{qB} i_{qB} = (1.141)(1.174)(1) = 1.340$.

In the L direction, the following quantities are found:

Eq. 7.29: $$d_{qL} = 1 + 2(0.9657)(1 - 0.6947)^2(0.2450) = 1.044$$

Eq. 7.11: $$i_{\gamma L} = \left[1 - 0.7\left(\frac{39}{108}\right)\right]^5 = 0.233$$

$$Li_{\gamma L} = 0.466$$

Eq. 7.10: $$i_{qL} = \left[1 - 0.5\left(\frac{39}{108}\right)\right]^5 = 0.3695$$

$$Li_{qL} = 0.739$$

Because $Bi_{\gamma B} > Li_{\gamma L}$, use Eq. 7.33 and the following computations.

Eq. 7.23: $$s_{\gamma L} = 1 - 0.49\left(\frac{0.466}{0.500}\right) = 0.627$$

Eq. 7.21: $$s_{qL} = 1 + 0.695\left(\frac{0.739}{0.500}\right) = 2.027$$

$$d_{qL}s_{qL}i_{qL} = (1.044)(2.027)(0.3695) = 0.782$$

$$d_{qB}s_{qB}i_{qB} = (1.141)(1.174)(1) = 1.340$$

Because $0.782 < 1.340$, use the lower q-term in Eq. 7.33.

$$Q_d = 1\left[\frac{1}{2}(0.95)(165.6)(2)(1)(0.627)(0.233) + (0.95)(0.5)(115.3)(1.044)(2.027)(0.3695)\right]$$

$$= 23.0 + 42.8 = 65.8 \text{ t}$$

In the first test noted above, the computed failure load was 108.8 t versus an experimental load of 180 t, yielding a factor of safety of 1.65 based on theory alone. In the second test, the computed failure load was 65.8 t versus an experimental load of 108 t, yielding a factor of safety of 1.64 based on theory alone.

Of interest is that Hansen employed a value of ϕ of 47°, instead of the 44° suggested by his equations, and obtained excellent agreement between the computed and experimental values of the failure load. Muhs and Weib (1969), as noted earlier, reported the measured friction angle to be between 40° and 42°. Had Hansen elected to use 42° instead of 40° for ϕ_{tr}, the value of ϕ_{pl} for use in the analytical computations would have been (42)(1.1) or 46.2 degrees, fairly close to the value that Hansen found to yield good agreement between experiment and analysis.

Ingra and Baecher (1983) discussed uncertainty in the bearing capacity of sands and concluded: ''When the friction angle is imprecisely known (e.g., having a standard deviation greater than l°), the effect of uncertainty in ϕ predominates other sources.''

Examples from Selig and McKee (1961) In contrast to the footings tested by Muhs and Weib (1969), Selig and McKee (1961) tested footings that ranged in size from 2 by 2 in. to 3 by 21 in. The soil employed was an Ottawa sand that was carefully placed to achieve a uniformity of 112.3 lb/ft^3 in a box that was 48 in. square by 36 in. deep. The friction angle of the sand was measured in the triaxial apparatus and was found to range from 38° to 41°. An average value of the friction angle was taken as 39.5; thus, using the

Hansen recommendation, the following value was computed for use in the analysis:

$$\phi_{pl} = 1.1\phi_{tr} = 43.45°$$

Some small footings were tested with no embedment, which is not consistent with practice. The experimental results greatly exceeded the results from analysis using the Hansen equations. Selig and McKee performed three tests where the base of the footings was placed below the ground surface. The following equation is solved in the table below, with the following constant values: $N_q = 106.0$; $N_\gamma = 149.2$; $\gamma = 0.0650$ lb/in.^{3}; $s_\gamma = 0.6$; $d_\gamma = 1.0$; $s_q = 1.688$; and d_q is as shown in the table.

$$\frac{Q_d}{A} = \frac{1}{2}\gamma B N_\gamma s_\gamma d_\gamma + \gamma D_f N_q s_q d_q$$

For the three experiments that were evaluated, the factors of safety in the equation that were computed in Table 7.2 were 1.50, 1.38, and 1.23, yielding an average value for a fairly small sample of 1.37. The selection of a value of ϕ_{pl} is important, and Hansen's correlation with ϕ_{tr} may be used unless a more precise correlation becomes available. A factor of safety appears in the Hansen procedure, as noted from the small sample, and additional analyses of experimental data of good quality, particularly with full-sized footings, will be useful.

The settlement at which failure is assumed to occur is of interest when performing experiments. With regard to the bearing capacity of the base of drilled shafts in sand, several experiments showed that the load kept increasing with increasing settlement, and it was decided that the ultimate experimental load could be taken at a settlement of 10% of the base diameter. A possible reason for the shape of the load-settlement curve was that the sand kept increasing in density with increasing settlement.

Muhs and Weib (1969) apparently adopted 25 mm as the settlement at which failure was defined. Only a few of the load-settlement curves were reported by Selig and McKee (1961), but those that were given showed failure to occur at a relatively small settlement, with the load remaining constant or decreasing after the maximum value was achieved. In both sets of experiments discussed above, the relative density of the sand was quite high, probably

TABLE 7.2 Computation of Q_d to Compare with Experimental Value

Footing size, in.	Area, in.^{2}	D_f, in.	d_q	Comp. Q_d, lb	Exp. Q_d, lb	Factor of Safety in Equation
3 × 3	9	2	1.123	261	391	1.50
3 × 3	9	4	1.171	516	711	1.38
3 × 3	9	6	1.205	782	964	1.23

leading to the maximum load at a relatively small settlement and a settlement-softening curve for greater settlement.

The small number of experiments where full-sized footings were loaded to failure is likely due to the cost of performing the tests. Furthermore, the cost of footings for a structure is likely to be small with respect to the cost of the entire structure, so the financial benefits of load tests would likely be small in most cases.

7.5 EQUATIONS FOR COMPUTING CONSOLIDATION SETTLEMENT OF SHALLOW FOUNDATIONS ON SATURATED CLAYS

7.5.1 Introduction

As noted earlier, the geotechnical design of shallow foundations is presented in Chapter 9. Two kinds of settlement are discussed: short-term or immediate settlement when the settlement of granular soils (sands) and cohesive soils (clays) will occur rapidly, and long-term settlement of clays that can occur over a period of years. Some long-term settlement of sands can occur. The most evident case is when the sands are subjected to vibration, causing the grains to move and increase the density of the soil. Large amounts of settlement can occur if very loose sands are subjected to vibration. Loose sands below the water table cannot rapidly increase in density when affected by an earthquake and are subject to liquefaction because the water cannot immediately flow out. When a stratum of sand is subjected to sustained loading, some settlement of the foundation may occur that is time dependent.

Long-term settlement of clay deposits below the water table is of concern to the geotechnical engineer. Two types of predictions must be made: the total settlement that can occur over a period of time and the time rate of settlement. The procedures available for making the two predictions are presented in the following sections.

The assumptions made to develop the equations for computing the total settlement of a stratum of saturated clay are as follows:

1. The voids in the clay are completely filled with water.
2. Both the water and the solids of the soil are incompressible.
3. Darcy's law is valid (see Chapter 3); the coefficient of permeability k is a constant.
4. The clay is confined laterally.
5. The effective and total normal stresses are the same for every point in any horizontal plane through the clay stratum during the process of consolidation (Terzaghi, 1943).

Further, Terzaghi noted that the process of consolidation, as water flows vertically though soil, is analogous to the heat flow from an infinite slab if

the slab is at a constant temperature and the boundaries are maintained at a different temperature.

If the assumptions noted above are correct, the equations for total settlement and the time rate of settlement of a stratum of clay below the water table when subjected to load are perfectly valid. The assumptions made in developing the theory cannot all be satisfied; for example, the loaded area must be finite, and some water could flow from the stratum laterally rather than vertically. However, if care is used in sampling and testing the stratum of clay, the consolidation equations can be used, as evidenced by past experience, to make predictions for the total settlement with reasonable accuracy and prediction of the time rate of settlement with less accuracy.

7.5.2 Prediction of Total Settlement Due to Loading of Clay Below the Water Table

Figure 7.9a shows a stratum of sand below the ground surface above a stratum of clay. The water table is shown in the stratum of sand. The assumption is made that the clay has always been saturated. The line labeled σ_0' shows the distribution of pressure from the self-weight of the soil prior to the imposition of a surface load, and the quantity $\Delta\sigma'$ shows the increase in σ' due to the surface loading. The curve in Figure 7.9b shows the results from a laboratory consolidation test of a sample of superior quality from the stratum of clay. The dashed line shows the direct results from the laboratory data, with the solid line showing the corrected laboratory curve to yield a field curve, as described in Chapter 3. The portion of the curves marked ''rebound'' indicates that the soil will swell when load is removed. The simple model for computing total settlement is shown in Figure 7.9c.

The determination of the change in void ratio Δe for use in computing settlement S is shown in Figure 7.9b The average value of $\Delta\sigma'$ shown in Figure 7.9a is added to σ_0', and the value of Δe is obtained as shown. The total settlement can now be computed with the equation in Figure 7.9c.

The equation for settlement S in Figure 7.9c may be rewritten in a convenient way to compute settlement based on the plot in Figure 7.10. The curve in the figure has been corrected to offset remolding and other disturbance. The plot of void ratio e versus the log of effective stress σ' is for a sample of clay that had been preloaded. The first branch of the curve indicates the reloading of the sample after removal of previous stress, the *reloading curve.* The other branch represents the behavior of the sample after exceeding the magnitude of the previous loading, the *virgin compression curve.* The equation for the two branches of the curve is as follows:

$$S = \frac{H}{1 + e_0}\left[c_r \log \frac{\sigma_p'}{\sigma_0'} + c_c \frac{\sigma_0' + \Delta\sigma'}{\sigma_p'}\right] \tag{7.36}$$

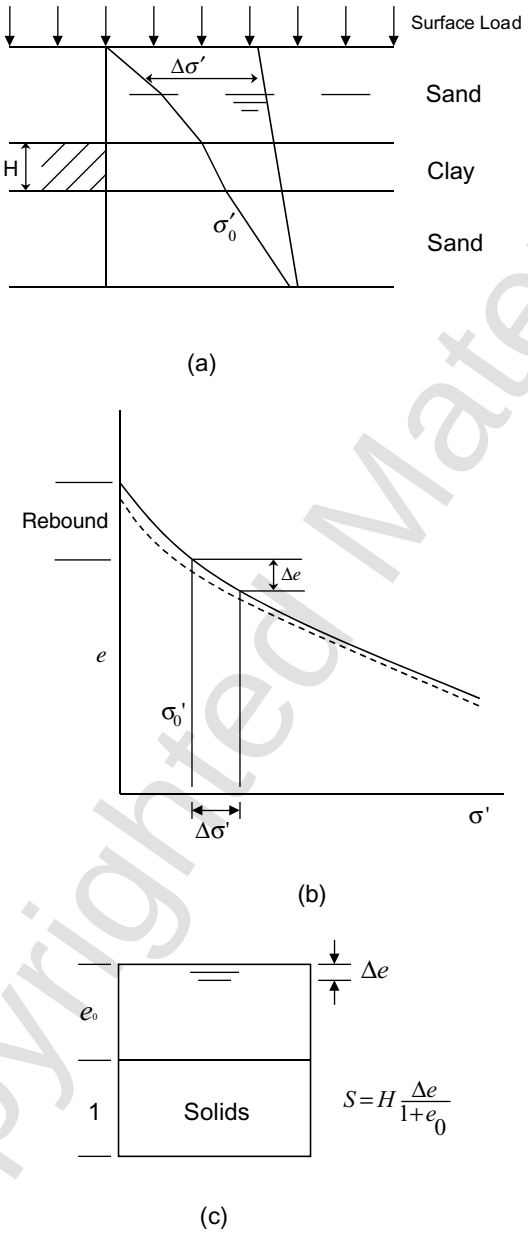

Figure 7.9 Data required for computing total settlement of a clay stratum due to an imposed surface load. (a) Solid profile showing initial effective stress σ'_0, surface load, and distribution of imposed load with depth $\Delta\sigma'$. (b) Field curve of void ratio e versus effective normal stress σ'. (c) Model for computing total settlement.

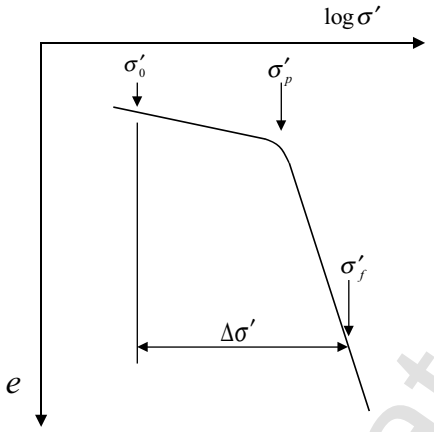

Figure 7.10 Plot of void ratio versus log of effective stress for an overconsolidated sample.

where

c_r = compression index (reloading), and
c_c = compression index (virgin loading), dimensionless.

In some instances, the settlement due to the reloading portion of the curves is deemed to be so small as to be negligible. For normally consolidated clay, only the virgin compression curve will be used.

To obtain the quantity $\Delta\sigma'$, a method for predicting the increase in load as a function of depth must be developed. An appropriate method has been proposed by Boussinesq (1885) as shown in the following equation (Terzaghi and Peck, 1948):

$$\sigma_v = \frac{3Q}{2\pi z^2}\left[\frac{1}{1 + (r/z)^2}\right]^{\frac{5}{2}} q \tag{7.37}$$

where

σ_v = stress in the vertical direction,
Q = concentrated vertical load,
z = vertical distance between a point N within an semi-infinite mass that is elastic, homogeneous, and isotropic, and
r = horizontal distance from point N to the line of action of the load.

The assumption is made that the applied load at the ground surface is perfectly flexible, with a unit load of q. The loaded area is divided into small parts, as

expressed in the following equation, where load dq is assumed to be acting at the centroid of the area dA:

$$dq = qdA \tag{7.38}$$

Substitution can be made into Equation 7.36 with the following result:

$$d\sigma_v = \frac{3q}{2\pi z^2}\left[\frac{1}{1 + (r/z)^2}\right]^{\frac{5}{2}} dA \tag{7.39}$$

The magnitude of σ_v at point N due the entire loaded area can be found by integrating Eq. 7.39. Newmark (1942) produced a chart for easy use in the determination of σ_v (Figure 7.11). The following procedure is employed in using the chart to find σ_v at depth z: the distance to the depth is given by the length A-B in the chart; employing the scale, a sketch is made of the loaded area; the point in the sketch under which the value of σ_v is desired is placed over the center of the sketch; the number of subdivisions n, including fractions, covered by the sketch is counted; and $\sigma_v = 0.005n\ \sigma_0$, where σ_0 is the vertical stress at the ground surface due to the applied load. The number of subdivisions in the chart is 200; therefore, if all of the subdivisions are covered, $\sigma_v = \sigma_0$.

Sketches of the loaded area are made for increasing depths using the A-B scale, with the sketches of the loaded area becoming smaller and smaller. Thus, a plot of σ_v as a function of depth z beneath the ground surface can readily be made. As shown in Figure 7.12, the value of σ_v as a function of depth z can readily be made for a point under a particular footing if a number of closely spaced areas exist with differing values of σ_0. The scale A-B was set at 8 ft; thus, the value of σ_v was to be determined at a depth of 8 ft below the base of the footings. As shown in Figure 7.12, the scale A-B was used to draw sketches of the footings 6 by 6 ft and 8 by 8 ft, separated by a distance of 3 ft. The value of σ_v was desired below the center of the smaller footing. As shown in the figure, the unit load on the smaller footing was 2 k/ft^2 and the load on the larger footing was 3 k/ft^2. The number of values of n under the smaller footing was 42.4, and n for the larger footing was 10.4. The value of σ_v can now be computed:

$$(\sigma_v)_{8\,ft} = (0.005)[(42.4)(2.0) + (10.4)(3.0)] = 0.424 + 0.156 = 0.58\ \text{k/ft}^2$$

Examining the plotting of the footing sizes in the figure shows that there was a lack of precision that had only a minor effect on the result. The Newmark chart can be used to obtain the increase in effective stress as a function of depth beneath a given point under a loaded area due to various horizontal spacings of footings, considering the surface loading from each of them.

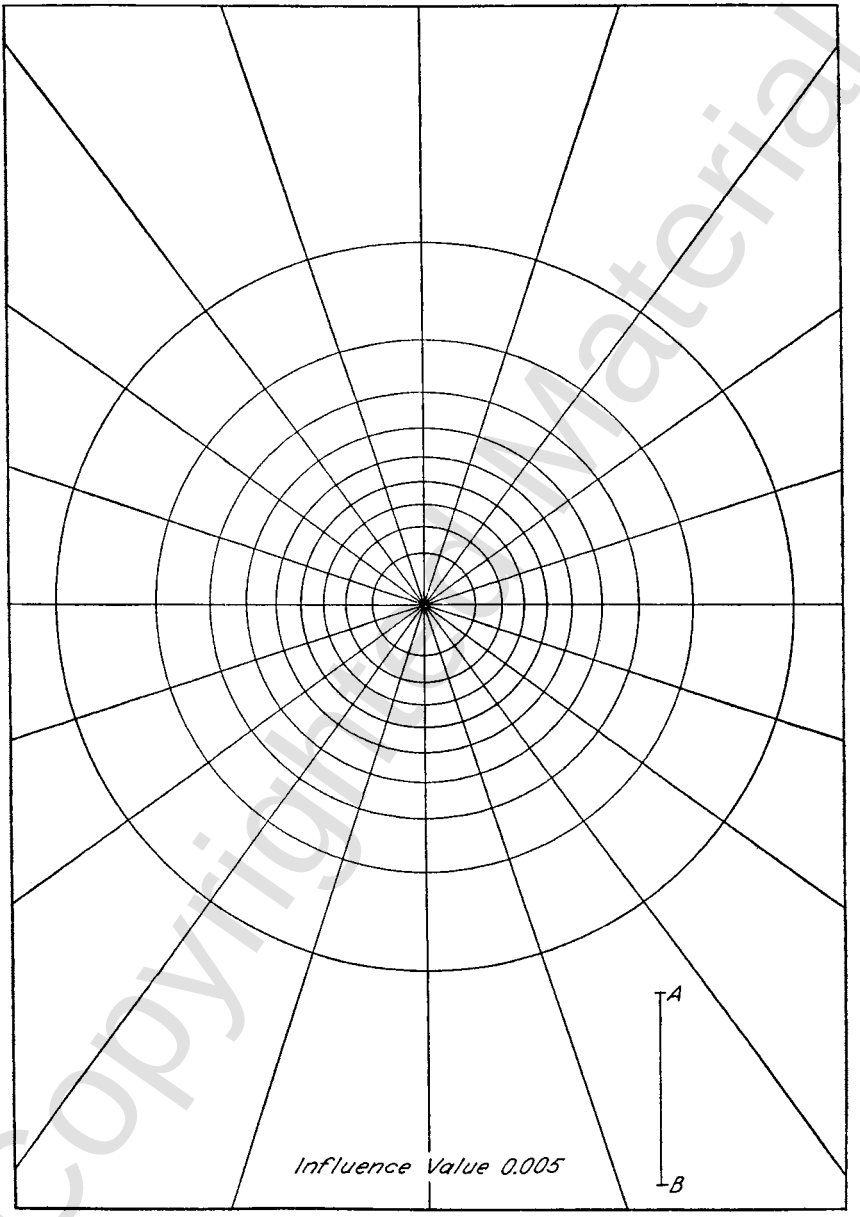

Figure 7.11 Newmark chart for computing vertical stress beneath a loaded area.

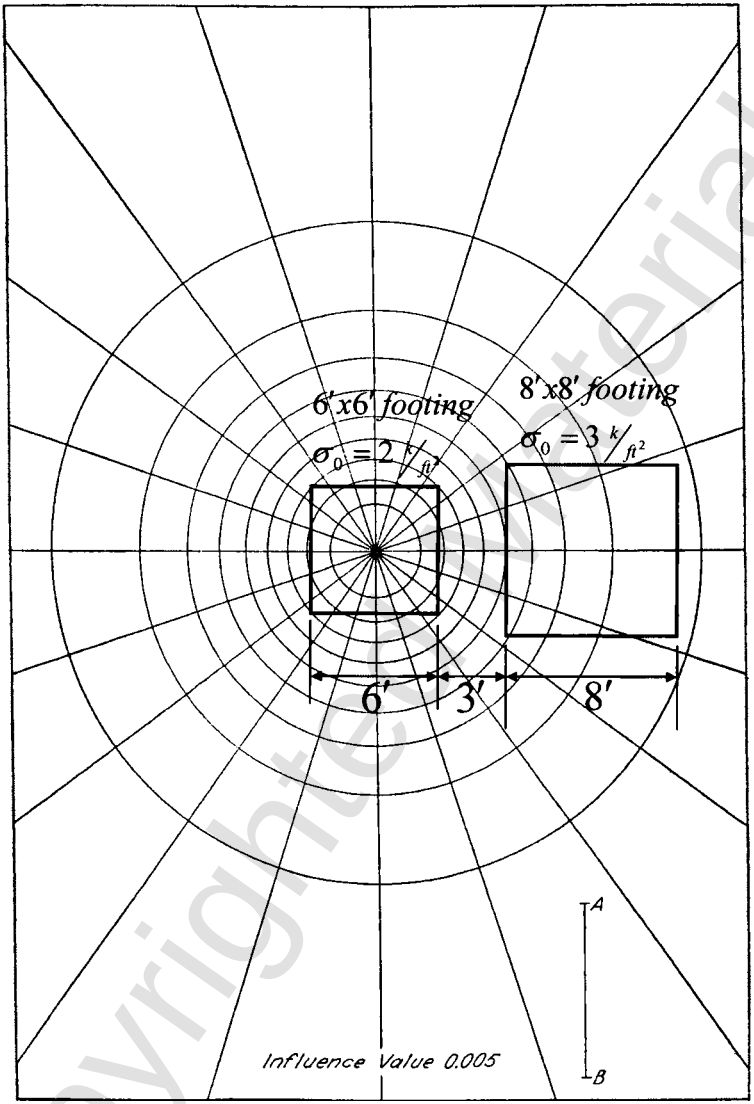

Figure 7.12 Example of use of the Newmark chart.

7.5.3 Prediction of Time Rate of Settlement Due to Loading of Clay Below the Water Table

Terzaghi (1943) reasoned that prediction of the time at which a certain amount of settlement occurs could be simplified by assuming that the surface loading occurred instantaneously, that excess porewater pressure would develop throughout the stratum of clay, and that drainage from the clay would occur

instantly where the clay interfaced with a porous stratum of sand. Thus, water in the stratum of clay in Figure 7.9 would drain upward from the top of the clay and downward from the bottom of the clay. Terzaghi noted that the process was precisely analogous to the heat-flow problem, where a semi-infinite slab of material at an elevated temperature is suddenly subjected to zero temperature, or to a lower temperature, at both surfaces of the slab.

The differential equation for heat flow is shown in Eq. 7.40 (Carslaw and Jaeger, (1947)

$$\frac{\partial u}{\partial t} = \kappa \frac{\partial^2 u}{\partial z^2} \tag{7.40}$$

where

u = temperature (excess porewater pressure), and
κ = diffusivity reflecting the ability of the slab of material to transmit heat.

The problem is to find the properties of the soil, plainly involving the coefficient of permeability k, that will replace the diffusivity κ. The term κ is replaced by c_v in consolidation theory, where c_v is called the *coefficient of consolidation,* as defined by the following equation:

$$c_v = \frac{k}{m_v \gamma_w} \tag{7.41}$$

where the rate of flow of water from the clay is directly proportional to the coefficient of permeability k and inversely proportional to γ_w and m_v, where $m_v = a_v/1 + e$ and $a_v = -de/d\sigma'$. Thus, if the *coefficient of compressibility,* a_v, is larger, meaning that the *coefficient of volume compressibility,* m_v, is larger, the rate of flow will be less. Thus, the differential equation for the rate at which water will flow from a stratum of clay that has been subjected to an increase in effective stress, σ', due to the placement of a surface loading above the clay, is shown in Eq. 7.42:

$$\frac{\partial u}{\partial t} = c_v \frac{\partial^2 u}{\partial t^2} \tag{7.42}$$

The solution of Eq. 7.41 requires the implementation of the following boundary conditions: the excess porewater pressure, u, is equal to zero at the drainage faces; the hydraulic gradient i is equal to zero at the mid-height of the stratum of clay and at the boundary where flow is prevented, where $i = du/dz$; and after a very long time (infinite according to the differential equation), $u = 0$ at all depths.

The solution of Eq. 7.42 for the conditions given is as follows:

$$U_z(\%) = f\left(T_v, \frac{z}{H}\right) \tag{7.43}$$

where

$$T_v = \frac{c_v}{H^2}\, t \tag{7.44}$$

The dimensionless number T_v is called the *time factor.* The solution of Eq. 7.43 in terms of dimensionless coefficients is shown in Figure 7.13. The figure illustrates the process of consolidation graphically by showing the distribution of excess porewater pressure, u, with the passage of time. The figure readily shows that a very long time will be required for u to equal zero throughout the stratum. The hydraulic gradient causing the discharge of porewater becomes smaller and smaller over time.

The data in Figure 7.13 can be integrated to produce Figure 7.14. The time for a given percentage of the consolidation to take place in the laboratory for a representative sample is determined, usually at 50% of the laboratory consolidation. Using the time factor T_v of 0.197 (see Figure 7.14), the value of the coefficient of consolidation c_v can be found. And Eq. 7.43 can be used to plot a curve showing the amount of settlement of the clay stratum as a function of time.

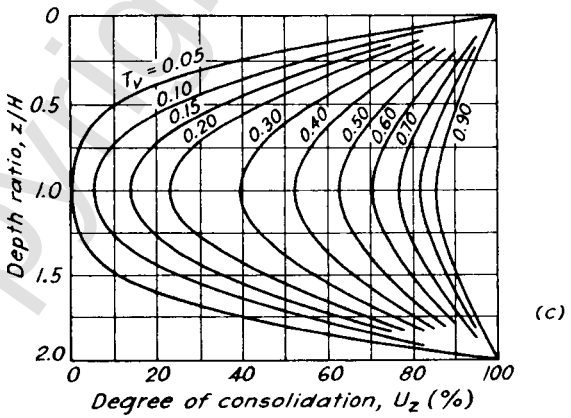

Figure 7.13 Percentage of consolidation U_z (%) as a function of relative depth Z/H and time factor T_v (note: thickness is 2H for the drainage top and bottom of the stratum) (from Peck et al., 1974).

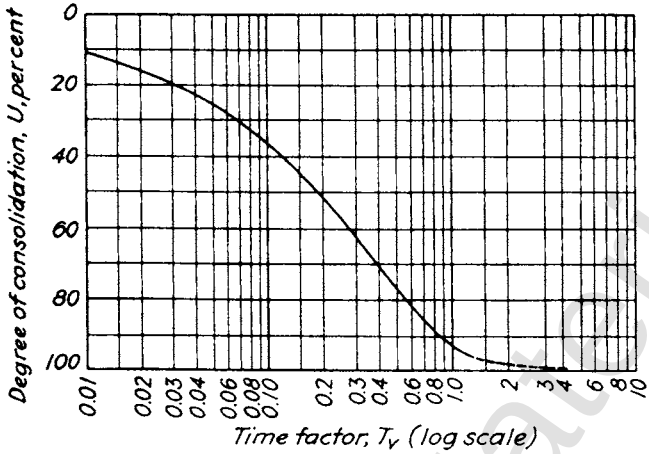

Figure 7.14 Theoretical relationship between degree of consolidation U and time factor T_v (from Peck et al., 1974).

PROBLEMS

P7.1. **a.** Compute the total load, Q_q, in kips, using the Hansen equations, for a footing 4 ft wide by 8 ft long founded on a stratum of sand. The vertical load is uniformly distributed; there is no horizontal load. The value of D_f is 3.5 ft, the water table is at the base of the footing, and the friction angle from the triaxial test is 30°. For the sand above the base of the footing, the water content is 20%, and the unit weight γ is 120 pcf. Compute a value of submerged unit weight γ' if needed, assuming specific gravity of the particles of sand to be 2.67.

b. The problem remains the same as in part a except that the footing rests on overconsolidated clay at a depth of 3.5 ft and the footing rests on the clay. Assume the same unit weights as before and determine the undrained shear strength of the clay to yield the value of Q_q found in part a.

P7.2. **a.** Under what condition might you wish to construct a footing with a base at some angle with the horizontal? Show a sketch.

b. What technique could you use to fine the most favorable angle for the base?

P7.3. Under what conditions would you wish to use the Hansen equations for a sloping ground? Show a sketch.

P7.4. The time to reach 55% consolidation for a laboratory sample of clay that was 0.6 in. thick and tested under double drainage was 24.5 seconds. How long would it take for a stratum of the same soil in the field that was 14 ft thick and drained on only one side to reach the same degree of consolidation?